No. DMR-8418846 and use of the Colorado State University Regional NMR Center, funded by NSF Grant No. CHE-8208821. We thank Dr. J. L. Kosmala and Dr. L. Winter of the 3M Corp. for supplying the fluorocarbon polymers.

Registry No. (HFP)(VF) (copolymer), 9011-17-0; (TFCE)(VF) (copolymer), 9010-75-7; (HFP)(TFE)(VF) (copolymer), 25190-89-0.

References and Notes

(1) Ferguson, R. C. *J. Am. Chem. Soc.* **1960**, *82*, 2416.
(2) Tiers, G. V. D.; Bovey, F. A. *J. Polym. Sci., Part A* **1963**, *1*, 833.
(3) Wilson, III, C. W.; Santee, E. R., Jr. *J. Polym. Sci., Part C* **1965**, *8*, 97.
(4) Naylor, R. E., Jr., Lasoski, S. W., Jr. *J. Polym. Sci.* **1960**, *44*, 1.
(5) Cais, R. E. *Macromolecules* **1980**, *13*, 806.
(6) Gerhardt, G. E.; Dumitru, E. T.; Lagow, R. J. *J. Polym. Sci., Polym. Chem. Ed.* **1979**, *18*, 157.
(7) Yagi, T. *Polym. J.* **1979**, *11*, 353.
(8) Tonelli, A. E.; Schilling, F. C.; Cais, R. E. *Macromolecules* **1982**, *15*, 849.
(9) Ferguson, R. C. *Kautsh. Gummi, Kunst.* **1965**, *11*, 723.
(10) Ishigure, K.; Watanabe, S.; Tabata, Y.; Oshima, K. *Macromolecules* **1980**, *13*, 1630.
(11) Ferguson, R. C.; Brame, E. G., Jr. *J. Phys. Chem.* **1979**, *83*, 1397.
(12) Hozumi, K.; Kitamura, K.; Kitade, T. *Bull. Chem. Soc. Jpn.* **1981**, *54*, 1392.
(13) Weigert, F. J. *Org. Magn. Reson.* **1971**, *3*, 373.
(14) English, A. D.; Garza, O. T. *Macromolecules* **1979**, *12*, 351.
(15) Yagi, T.; Tatemoto, M. *Polym. J.* **1979**, *11*, 429.
(16) Ishigure, K.; Tabata, Y.; Oshima, K. *Macromolecules* **1970**, *3*, 27.
(17) Murasheva, Y. M.; Shashkov, A. S.; Dontsov, A. A. *Polym. Sci. USSR (Engl. Transl.)* **1981**, *23*, 711.
(18) Murasheva, Y. M.; Shashkov, A. S.; Galil-Ogly, F. A. *Polym. Sci. USSR (Engl. Transl.)* **1980**, *21*, 968.
(19) Smith, P.; Gardner, K. H. *Macromolecules* **1985**, *18*, 1222.
(20) Mehring, M. *High-Resolution NMR Spectroscopy in Solids. NMR, Basic Principles and Progress*; Diehl, P., Fluck, E., Kosfeld, R., Eds.; Springer-Verlag: New York, 1976.
(21) Mehring, M.; Griffin, G. R.; Waugh, J. S. *J. Chem. Phys.* **1971**, *55*, 746.
(22) English, A. D.; Vega, A. J. *Macromolecules* **1979**, *12*, 353.
(23) Yesinowski, J. P.; Mobley, M. J. *J. Am. Chem. Soc.* **1983**, *105*, 6191.
(24) Gerstein, B. C.; Dybowski, C. R. *Transient Techniques in NMR of Solids*; Academic: New York, 1985.
(25) Maricq, M. M.; Waugh, J. S. *J. Chem. Phys.* **1979**, *70*, 3300.
(26) Dec, S. F.; Wind, R. A.; Maciel, G. E.; Anthonio, F. E. *J. Magn. Reson.* **1986**, *70*, 355.
(27) Dr. J. L. Kosmala and Dr. L. Winter kindly provided the samples as well as information on the monomer components and compositions, where known.
(28) Wind, R. A.; Anthonio, F. E.; Duijvestijn, M. J.; Smidt, J.; Trommel, J.; DeVette, G. M. C. *J. Magn. Reson.* **1983**, *52*, 424.
(29) Andrew, E. R. *Int. Rev. Phys. Chem.* **1981**, *1*, 195.
(30) Dungan, C. H.; Van Wazer, J. R. *Compilation of Reported F^{19} NMR Chemical Shifts*; Wiley-Interscience: New York, 1970.
(31) Kessemeier, H.; Norberg, R. E. *Phys. Rev.* **1967**, *155*, 321.
(32) Koenig, J. L. *Chemical Microstructure of Polymer Chains*, Wiley-Interscience: New York, 1980.

Pulsed Dynamic NMR of Fibers from Thermotropic Liquid-Crystal Polymers

Klaus Müller, Andreas Schleicher, Ernst Ohmes, Alberta Ferrarini,[†] and Gerd Kothe*

Institut für Physikalische Chemie, Universität Stuttgart, Pfaffenwaldring 55, D-7000 Stuttgart 80, West Germany. *Received March 17, 1987*

ABSTRACT: Semiflexible liquid-crystal polyesters were melt spun into highly oriented fibers with tensile moduli up to $E = 22$ GPa and studied by pulsed dynamic NMR techniques. Analysis of the various ^{2}H NMR experiments provided detailed information about molecular order and dynamics of these systems. As-spun and annealed fibers are characterized by a high degree of orientational and conformational order of the polymer chains. In addition, practically all director axes are aligned in draw direction. High modulus and strength result from these highly oriented chain configurations. Molecular motion in annealed fibers is heterogeneous, as two components are detected. One component exhibits similar fast dynamics as observed in the anisotropic melt (liquid-crystalline phase), while the other shows a drastic motional decrease (crystalline phase). Decomposition of various NMR relaxation curves into two components yields a crystallinity of (55 ± 5)%, subject to the annealing conditions. However, the degree of order is independent of the thermal history, in agreement with only subtle changes of the mechanical properties upon annealing.

Introduction

Thermotropic liquid-crystal main-chain polymers (LCPs) have attracted considerable attention within the last years. This is due to their ease in melt processing and expected good mechanical properties which suggest potential application as high-modulus fibers and moldings.[1-3] From the chemical point of view three basic types of polymers can be distinguished: (i) rigid homopolymers, (ii) random copolymers, and (iii) semiflexible homopolymers.

Completely rigid homopolymers often exhibit lyotropic mesophases in the presence of a suitable solvent. The lack of thermotropic mesomorphism for these systems is attributed to the undesirable high melting temperatures being higher than the corresponding decomposition temperatures.[4] Thus, the reduction of the melting temperature is the main objective in getting thermotropic LCPs with stable mesophases. This can be achieved either by random rigid copolymers[5] or by semiflexible homopolymers having alternating rigid and flexible residues within the repeating unit.[6] In recent years both types of LCPs have been investigated in detail. In particular, pulsed dynamic NMR of deuteron (^{2}H) labeled polymers has successfully been employed for a comprehensive molecular characterization of these systems.[7]

Although melt spinning data and fiber studies for a number of thermotropic copolymers have been reported,[8-10] only limited information about fibers of semiflexible homopolymers is available.[11,12] In this paper we present pulsed ^{2}H NMR studies of melt spun fibers from nematic polyesters, containing a flexible spacer. Variation of pulse sequence and pulse separation provides the large number

---

[†] Present address: Istituto di Chimica Fisica, Università di Padova, Via Loredan, I-35100 Padova, Italy.

0024-9297/87/2220-2761$01.50/0 © 1987 American Chemical Society

of independent experiments, necessary for a proper molecular characterization of these systems.

In the first section the theoretical background is presented. The theory is then applied to the analysis of dynamic ^{2}H NMR experiments of LCP fibers from specifically deuteriated polyesters having a repeating unit such as I. Computer simulations provide the orientational distributions and conformations of the polymer chains and the correlation times of the various motions. They are related to molecular order and dynamics of the LCP fibers.

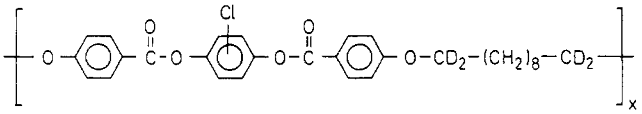

I

For comparison thermodynamic and mechanical properties have been studied. The results, referring to as-spun and annealed fibers, are discussed in relation to the molecular properties, evaluated by the NMR experiments. The discussion clearly demonstrates the advantages of pulsed dynamic NMR in characterizing new materials such as LCP fibers.

NMR Theory

Pulsed dynamic NMR of specifically deuteriated compounds has been established as a powerful tool to study molecular order and dynamics in complex chemical systems.[7,13,14] The deuterons, exhibiting isolated magnetic interactions, serve as reliable probe nuclei for the molecular environment. Generally, the ^{2}H labeled system is subject to a sequence of nonselective radiofrequency pulses and the response after the last pulse is used to evaluate the molecular properties of the system. By using different pulse sequences, the various molecular motions can be differentiated over a wide dynamic range, extending from the fast rotational to the ultraslow motional regime. In addition, various types of molecular order, modulated by the different motions, are discriminated, likewise.

Analysis of these pulsed NMR experiments is conveniently achieved by employing a density matrix treatment, developed previously.[7,15] The action of the different pulses on the time-dependent spin density matrix $\rho(t)$ is considered by employing Wigner rotation matrices. Between the pulses the density matrix is assumed to obey the stochastic Liouville equation[16,17]

$$\frac{\partial}{\partial t}\rho(\Omega,t) = -(i/\hbar)\mathbf{H}^x(\Omega)\cdot\rho(\Omega,t) - \Gamma_\Omega\cdot[\rho(\Omega,t) - \rho_{eq}(\Omega)] \quad (1)$$

which we solve using a finite grid point method.[18,19] Here $\mathbf{H}^x(\Omega)$ is the Hamiltonian superoperator of the spin system, depending on the orientation and conformation of the molecule specified by its Euler angles Ω. Γ_Ω is the time-independent Markov operator for the various rotational processes and $\rho_{eq}(\Omega)$ is the equilibrium density matrix.

In the finite grid point method[18,19] the Markov operator is represented by a matric $\mathbf{W}(\Omega,\Omega)$ whose elements give the transition rates between discrete sites of Ω. The values of the transition rates depend upon the model used to describe the motion. For the intermolecular motion (overall motion of the polymer chain) a continuous diffusive process is assumed. In that case the elements of $\mathbf{W}(\Omega,\Omega)$ must satisfy the following equations[19]

$$\begin{aligned} W(\Omega_m,\Omega_{m+1}) + W(\Omega_m,\Omega_{m-1}) &= (3\Delta^2\tau_R)^{-1} \\ W(\Omega_m,\Omega_n)P_{eq}(\Omega_m) &= W(\Omega_n,\Omega_m)P_{eq}(\Omega_n) \\ W(\Omega_m,\Omega_m) &= -(3\Delta^2\tau_R)^{-1} \end{aligned} \quad (2)$$

where Δ is the angular separation of adjacent grid points. Solving eq 2, one can establish values for all intermolecular transition rates in terms of two rotational correlation times $\tau_{R\perp}$ and $\tau_{R\parallel}$ and the equilibrium population $\mathbf{P}_{eq}(\Omega)$ of the sites; $\tau_{R\perp}$ is the correlation time for reorientation of the symmetry axis of the diffusion tensor, while $\tau_{R\parallel}$ refers to rotation about this axis.

For the intramolecular motion (trans-gauche isomerization of the chain) a random jump process is assumed. Consequently, the intramolecular transition rates are given by

$$W(\Omega_m,\Omega_n) = (1/\tau_J)[P_{eq}(\Omega_n) - \delta_{mn}] \quad (3)$$

where τ_J is the average residence time in one conformation.

The equilibrium distribution $\mathbf{P}_{eq}(\Omega)$ is described in terms of internal and external coordinates. The internal part accounts for different conformations and the external part for different orientations. Generally, there are only four conformational states for a particular aliphatic chain segment.[20] The corresponding populations n_1, n_2, n_3, and n_4 may be used to set up a segmental order matrix, which on diagonalization yields the segmental order parameters $S_{Z'Z'}$ and $S_{X'X'} - S_{Y'Y'}$.[15] They express the ordering of the most-ordered segmental axis Z' and the anisotropy of that order, respectively.

The external part of the equilibrium distribution of the chain molecules is described in the mean-field approximation, using an orienting potential such as is common in molecular theories of liquid crystals.[21] In case of axial symmetry only two parameters, A and B, enter the orientational distribution function.[7,15] The coefficient A characterizes the orientation of the chain molecules with respect to a local director (microorder), while the parameter B specifies the orientation of the director axes in a laboratory frame (macroorder). The orientational micro- and macroorder parameters S_{ZZ} and $S_{z''z''}$ are related to the coefficients A and B by mean-value integrals:[22]

$$\begin{aligned} S_{ZZ} &= (1/2)N_1\int_0^\pi (3\cos^2\beta - 1)\exp(A\cos^2\beta)\sin\beta\,d\beta \\ S_{z''z''} &= (1/2)N_2\int_0^\pi (3\cos^2\delta - 1)\exp(B\cos^2\delta)\sin\delta\,d\delta \end{aligned} \quad (4)$$

Experimental Section

Materials. The specifically deuteriated polyester poly[1-[4-[[4-[(4-oxybenzoyl)oxy]chlorophenoxy]carbonyl]phenoxy]-1,1,10,10-tetradeuteriodecane] (I) was prepared by solution polymerization of 1,10-bis[4-(chloroformyl)phenoxy]decane-*1,1,10,10-d$_4$*[23] and chlorohydrochinon as described elsewhere.[24,25] Average molecular weights $\bar{M}_n$ of the samples were determined by vapor pressure osmometry using tetrachloroethane as solvent. The phase behavior of the polymer samples was investigated by differential scanning calorimetry (Perkin-Elmer DSC 7) and polarization microscopy (Leitz Ortholux II, Linkham THM 600 hot stage). Table I lists relevant thermodynamic properties of the systems studied. Note that both samples exhibit a stable nematic melt over a large temperature range (≥100 K).

Fiber Spinning. Preparation of the fibers was achieved by using a melt spinning unit (E. Blaschke). The piston-type extruder operated at constant velocity with a conical die having a length of 11 mm and a diameter of 3 mm (entrance). The narrow cylindrical outlet of the die was 400 μm in length with a diameter of 400 μm. In all cases extrusion rates of V_0 = 2.5 m/min were employed. The spinning temperatures are summarized in Table II. Fibers were extruded in air at ambient temperatures and collected on a bobbin (diameter 90 mm), placed 1 m from the extruder die. Generally, the spin-draw ratio was $V_t/V_0 = 50$, where V_t is the take-up velocity. All fibers were stored at room temperature. Annealing was performed by employing the various conditions given below. The amount of polymer for each spinning experiment varied between 4 and 6 g.

Table I
Thermodynamic Properties of the Liquid-Crystal Polymers Studied

		phase transitn temp[b]			transitn enthalpies[c]	
polymer	$\bar{M}_n$[a]	T_g	T_m	T_{ni}	ΔH_m	ΔH_{ni}
Ia	10 000	313	443	554	8.6	12.7
Ib	30 000	313	450	567	7.8	13.5

[a] Molecular weight; determined by vapor pressure osmometry. [b] In K; determined by DSC; scanning rate, 10 K/min. g = glass; m = melt; n = nematic; i = isotropic. [c] In J/g; determined by DSC.

Mechanical Measurements. Young's modulus (E), tensile strength (T), and elongation to break (ϵ) of as-spun and annealed fibers were evaluated from stress–strain curves measured by using a Textechno machine (Type Statimat). All measurements were performed at room temperature on single filaments about 25 cm long. The results, summarized in Table II, represent averages over at least five individual determinations. Annealed fibers for the mechanical measurements were obtained by heat treatment at 373 K for 2 h and at 373 K < $T \leq$ 423 K for 7 h.

NMR Measurements. The ^{2}H NMR measurements were performed on a Bruker CXP 300 pulse spectrometer at 46.1 MHz (B_0 = 7 T), using quadrupole echo[26-28] ($(\pi/2)_x$–τ_1–$(\pi/2)_y$) and saturation recovery sequences[29] ($(\pi/2)$–τ_1–$(\pi/2)_x$–τ_2–$(\pi/2)_y$). The width for a $\pi/2$ pulse was 3.5 μs, employing a home-built probe, equipped with a goniometer. If necessary, line shapes were corrected for distortion which is caused by using a finite pulse width.[30,31] All experiments were recorded by using quadrature detection with a digitizing rate of 2 MHz and appropriate phase cycling schemes. The number of scans varied between 1000 and 10 000 (200 mg of deuteriated material).

Annealed fibers for the NMR experiments were obtained by heat treatment at 413 K for about 40 min. No change in the NMR spectra was observed upon further annealing.

NMR Data Analysis. A Fortran program package was employed to analyze the ^{2}H NMR measurements.[7,15] The programs simulate pulsed dynamic NMR experiments of I = 1 spin systems undergoing inter- and intramolecular motion in an anisotropic medium. Numerical solution of the stochastic Liouville equation was achieved using the Rutishauser[32] or more efficiently the Lanczos algorithm.[33] Within the Redfield limit[34] analytical solutions are available. All programs were run on a Hewlett-Packard 1000 computer (F series, 1.2 Mbyte memory).

The constant parameters in the calculations were obtained from fast rotational and rigid limit quadrupole echo spectra of the bulk polymers. As found previously, the quadrupole coupling constant of the aliphatic deuterons is e^2qQ/h = 165 kHz.[7]

Analysis of the ^{2}H NMR experiments requires a knowledge of the orientation of the various molecular tensors in polymer I. Angular dependent ^{2}H NMR studies of macroscopically aligned samples indicate that each repeating unit can be characterized by a single-order tensor axially symmetric along Z.[7] Within the limits of error, the tilt angle ϑ'' between Z and the aliphatic chain axis Z'' is 0° ≤ 10°.[7,35] This finding corresponds to the overall shape of the chain molecule which is also expected to exhibit axially symmetric rotational diffusion about the Z axis.

An iterative fit of several angular and pulse-dependent ^{2}H NMR experiments for any given temperature provided reliable values for the simulation parameters, i.e., the parameters of conformational ($S_{Z'Z'}$) and orientational order (S_{ZZ}, $S_{z''z''}$) and the correlation times of the various types of motion ($\tau_{R\parallel}$, $\tau_{R\perp}$, τ_J). Details of this analysis are given elsewhere.[7,15]

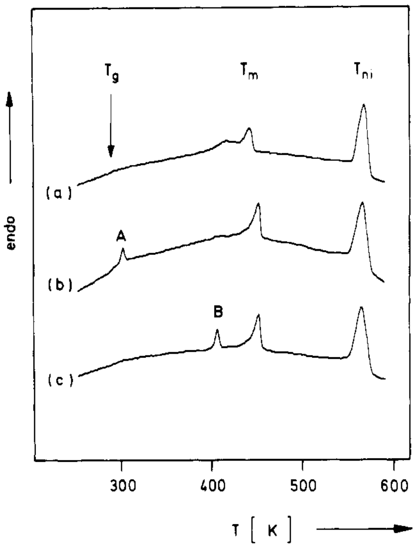

Figure 1. DSC traces of the liquid-crystal polymer Ib at different thermal histories: (a) as-received polymer during second heating run; (b) as-spun fibers (T_s = 483 K), kept at room temperatures for several days; (c) annealed fibers (T_s = 483 K) after heat treatment at 403 K for 40 min. The heating rate is 10 K/min.

Results

Thermal Behavior. Representative DSC thermograms of the LCP Ib are shown in Figure 1. The DSC curve (second run) of the as-received polymer (trace a), i.e., unprocessed material, displays the typical feature of a semicrystalline polymer with a glass transition (T_g) and a melting peak (T_m) from the solid state to the anisotropic melt. An additional endotherm at T_{ni} reflects the phase transition to the isotropic melt. It is interesting to note that the clearing enthalpy is larger than the corresponding enthalpy of fusion (see Table I), in contrast to observations on low molecular weight liquid crystals.

At first glance, the DSC thermogram of the as-spun fibers, given in trace b, is rather similar to that of the as-received polymer. However, closer inspection reveals that the melting peak is affected by the sample history, showing a positive temperature shift of about 10 K and a slightly reduced peak area upon melt spinning. In addition, a further low-temperature endotherm (A) is observed just above T_g in the thermogram of the as-spun fibers. Quenching experiments of as-received polymers suggest that this peak is due to an annealing process at room temperature. In the DSC thermograms recorded immediately after the quenching experiments a normal glass transition is observed. However, DSC curves of quenched samples, kept at room temperature for several days, display the same endotherm near T_g as found for the as-spun fibers.

Table II
Molecular and Mechanical Properties of the LCP Fibers Studied

		spinning temp,[a]		order parameters[c]			mechanical properts[d]		
polymer	mol wt $\bar{M}_n$	$T_s - T_m$	crystallin.[b]	$S_{Z'Z'}$	S_{ZZ}	$S_{z''z''}$	E	T	ϵ
Ia	10 000	15	55	0.7 (0.75)	0.9	0.9	11.0	0.14	2.5
Ia	10 000	10	55	0.7 (0.75)	0.9	0.9	11.4	0.15	2.5
Ib	30 000	33	55	0.7 (0.75)	0.9	0.9	10.7	0.31	2.5
Ib	30 000	18	55	0.7 (0.75)	0.9	0.9	11.4	0.32	2.5
Ib	30 000	8	55	0.7 (0.75)	0.9	>0.95	22.0	0.34	2.5

[a] In K; T_s = spinning temperature; T_m = melting point. [b] Crystallinity in percent. [c] For definition of order parameters see NMR Theory; values in brackets refer to crystalline component; $S_{Z'Z'}$ = segmental order parameter (α-segment); S_{ZZ} = orientational order parameter; $S_{z''z''}$ = degree of alignment of director axes. [d] Young's modulus (E), tensile strength (T) in GPa, and elongation to break (ϵ) in percent.

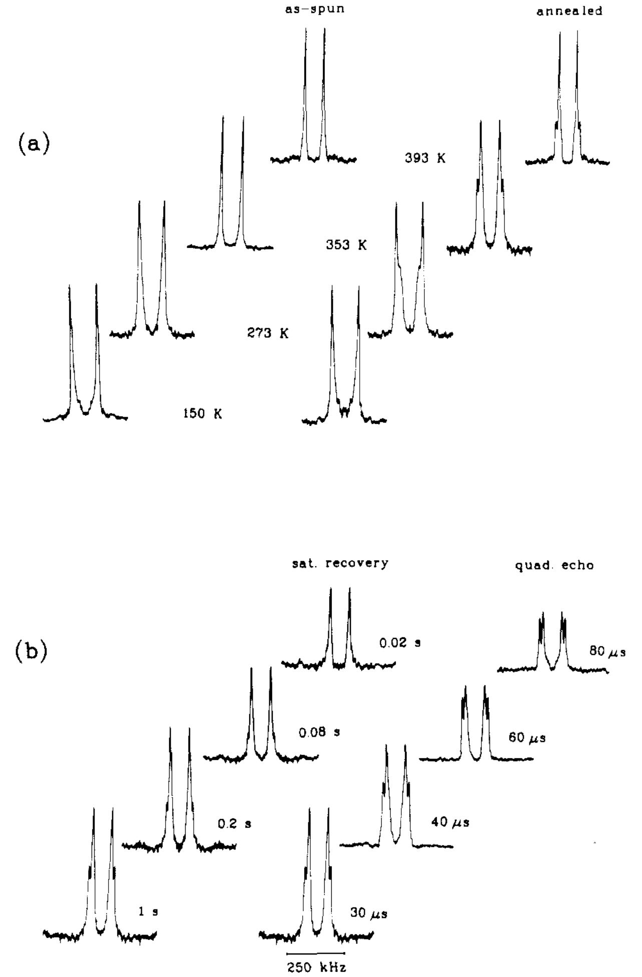

Figure 2. Experimental ^{2}H NMR spectra of fibers from liquid-crystal polymer Ib (T_s = 458 K) at parallel orientation of fiber axis and magnetic field. (a) Quadrupole echo spectra (pulse separation τ_1 = 30 μs) at four different temperatures. Left row: as-spun fibers. Right row: annealed fibers. All spectra are scaled to the same height. (b) Partially relaxed spectra (T = 353 K) at different pulse separation times τ_1. Left row: saturation recovery sequence. Right row: quadrupole echo sequence. All spectra reflect the actual intensity in the particular sequence.

The DSC curve of the annealed fibers (trace c) again shows an interesting feature. Here, instead of the endotherm near T_g, an endothermic peak (B) approximately 15 K above the annealing temperature is observed. The peak area and thus the enthalpy value increases with annealing time to a limiting value of about $\Delta H_m/4$. However, the original high-temperature melting peak is not affected by the heat treatment as can be deduced from the diagram.

NMR Line Shapes and Relaxation. Melt spun fibers of the specifically deuteriated LCP I have been studied over a wide temperature range (130 K $\leq T \leq$ 393 K), using pulsed dynamic NMR techniques. Representative results for as-spun and annealed fibers are shown in Figures 2–4. The observed ^{2}H NMR line shapes and relaxation curves, varying drastically with magnetic field orientation, demonstrate the power of the method.

Figure 2a shows quadrupole echo line shapes of as-spun (left row) and annealed fibers (right now) at four different temperatures. The ^{2}H NMR spectra refer to parallel orientation of fiber axis and magnetic field. Depending on the thermal history, characteristic differences are observed. The spectra of the as-spun fibers exhibit a single splitting over the whole temperature range investigated. In contrast, the line shapes of the annealed fibers indicate two overlapping components associated with mobile and immobile deuterons in distinct regions of the polymer. At the lowest temperature, the two fractions cannot be separated from the line shape anymore.

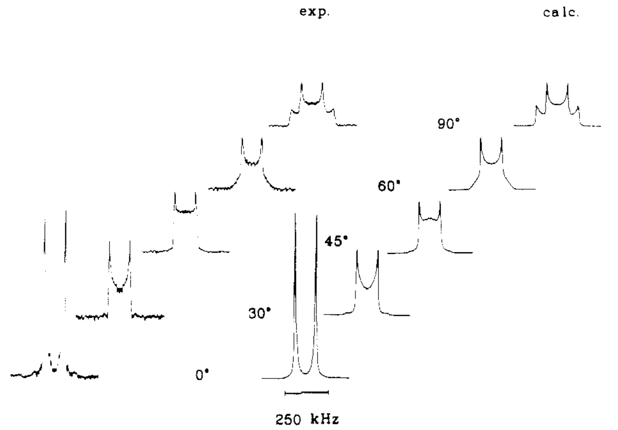

Figure 3. Experimental and calculated ^{2}H NMR spectra of annealed fibers from liquid-crystal polymer Ib (T_s = 458 K) at T = 130 K and five different angles between fiber axis and magnetic field. The spectra refer to quadrupole echo sequences and a fixed pulse separation of τ_1 = 30 μs. Calculations were obtained with $S_{Z'Z'}$ = 0.7 (0.75), S_{ZZ} = 0.9, $S_{z''z''}$ = 1.0, and $\tau_{\text{R}\perp} = \tau_{\text{R}\parallel} > 10^{-3}$ s, $\tau_J = 10^{-4}$ s (10^{-4} s). The values in brackets refer to the immobile component with a mole fraction of 0.55. Note that all spectra are normalized to the same total intensity.

Figure 2b shows partially relaxed ^{2}H NMR spectra of annealed fibers of LCP I at four different pulse separations τ_1 in a saturation recovery (left row) and a quadrupole echo sequence (right row). The spectra refer to the same temperature (T = 353 K) and parallel orientation of fiber axis and magnetic field. Again two spectral components are observed. The central peaks refer to the mobile fraction of the polymer while the outer peaks correspond to the immobile part. One recognizes that with increasing τ_1 significant spectral changes occur, resulting from different spin–lattice relaxation times T_{1Z} (left row) and spin–spin relaxation times T_{2E} (right row). Apparently, the mobile fraction relaxes somewhat faster than the immobile one.

Figure 3 (left row) depicts the angular variation of the quadrupole echo line shapes at T = 130 K. The spectra refer to annealed fibers and five different orientations of fiber axis and magnetic field. Drastic spectral changes are observed when the sample is rotated. A detailed analysis (right-row spectra) reveals that spinning from the anisotropic melt produces highly ordered fibers with nearly perfect alignment of the director axes.

In Figure 4 the spin–lattice relaxation times T_{1Z} (full and open squares) and the spin–spin relaxation times T_{2E} (full circles) are plotted as a function of $1/T$. All relaxation times refer to annealed fibers and parallel orientation of fiber axis and magnetic field. The values of T_{1Z} were obtained by recording the echo amplitude of a saturation recovery sequence as a function of τ_1 and by decomposing this function into two exponentials. One sees that the spin–lattice relaxation times of the mobile ($T_{1Z}{}^{\text{m}}$) and immobile fraction ($T_{1Z}{}^{\text{im}}$) differ by a factor of 10–50. Decomposition of the various relaxation curves into two components yields an immobile fraction of (55 ± 5)%. Note, however, that the corresponding decay curves of as-spun fibers cannot be separated into different components anymore.

The spin–spin relaxation times T_{2E} were obtained from the decay of the echo amplitude in a quadrupole echo sequence. Since a *unique* decomposition into two exponentials was impossible the given T_{2E} data represent bulk relaxation times and refer to both mobile and immobile deuterons. Generally, T_{2E} is defined as the time it takes

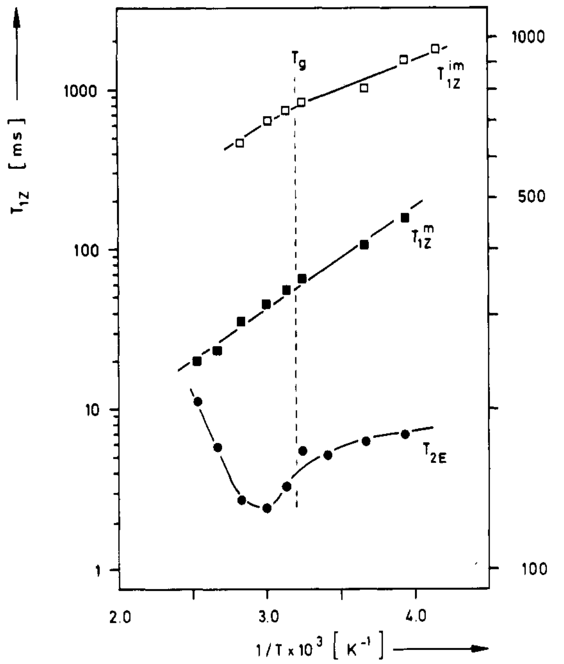

Figure 4. Temperature dependence of ^2H spin relaxation times of annealed fibers from liquid-crystal polymer Ib (T_s = 458 K). All relaxation times refer to parallel orientation of fiber axis and magnetic field. Left ordinate scale: spin–lattice relaxation times T_{1Z} (full and open squares). Right ordinate scale: spin–spin relaxation times T_{2E} (full circles). T_{1Z}^{m} refers to the mobile component and T_{1Z}^{im} refers to the immobile component, while T_{2E} represents a bulk relaxation time which is an average for mobile and immobile deuterons. The solid lines are best-fit simulations of the relaxation times, employing the NMR model of the Theory section and the parameters of Figure 5 and Table II. T_g = glassy point as determined by DSC.

for the echo amplitude to decay to $1/e$ of its original value. Note, the T_{2E} first decreases with decreasing temperature, then passes through a minimum at T = 333 K, and finally increases again. This striking behavior, expected on theoretical grounds, has also been observed in a lyotropic liquid crystal.[15]

Quantitative data concerning molecular order and dynamics of the LCP fibers were obtained by computer simulation of the various NMR experiments employing the NMR model outlined above. In the following we would like to describe the results in more detail, treating the various simulation parameters separately.

Motional Correlation Times. In Figure 5 the correlation times of the various motions in annealed fibers of LCP I are plotted as a function of $1/T$. They refer to reorientation of the chain axis (circles), rotation about the chain axis (triangles), and trans–gauche isomerization (squares) of the outer spacer segment. Inspection of the logarithmic plot reveals a surprisingly fast dynamic range, extending from 10^{-8} to 10^{-4} s.

As mentioned above the annealed fibers appear to be heterogeneous, as two components (mobile and immobile deuterons) are detected in the NMR experiments. Diffusive motions of larger chain segments and local conformational changes contribute to the dynamics of the mobile component. In contrast, only restricted local motions are observed for the immobile fraction, exhibiting slow trans–gauche isomerization in the range of $\tau_J \cong 10^{-6}$ s.

The activation energies for trans–gauche isomerization of E_J = 16 kJ/mol (mobile component) and E_J = 6.7 kJ/mol (immobile component) correspond to the local character of this motion. Higher activation energies of $E_{R\parallel}$ = 48 kJ/mol and $E_{R\perp}$ = 53 kJ/mol are observed for chain rotation and chain fluctuation in the mobile fraction.

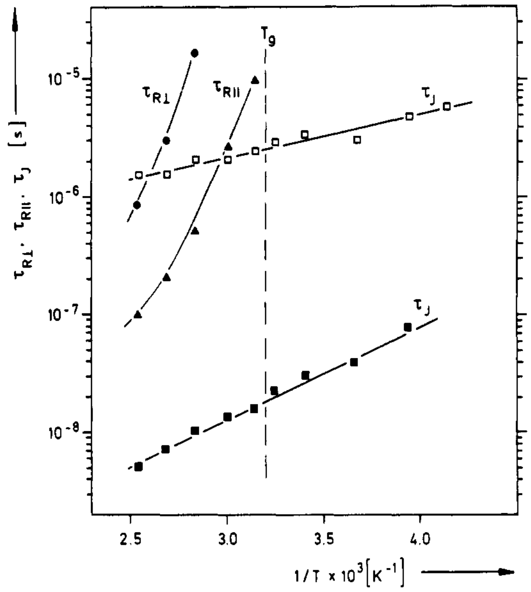

Figure 5. Arrhenius plot of the various correlation times characterizing the molecular dynamics of fibers from liquid-crystal polymers Ib (T_s = 458 K). Circles refer to chain fluctuations ($\tau_{R\perp}$), triangles denote chain rotation ($\tau_{R\parallel}$), and squares denote trans–gauche isomerization (τ_J). Mobile and immobile components are distinguished by full and open symbols. T_g = glassy point as determined by DSC.

Order Parameters. Molecular order of the LCP fibers is conveniently described in terms of three different order parameters $S_{Z'Z'}$, S_{ZZ}, and $S_{z''z''}$, characterizing (i) the segmental order of a particular spacer segment, (ii) the orientational order of the mesogenic units, and (iii) the alignment of the director axes. The measurement of these parameters is important for relating macroscopic physical properties of the LCP fibers to their molecular structure. Various static methods have been used to measure order parameters in these systems, but these methods are unable to essentially separate the three types of molecular order.

Pulsed dynamic NMR techniques do not suffer from this deficiency. Unequivocal determination of the various order parameters is always possible, provided the molecular motion is fast. Table II summarizes the results for LCP I. They refer to as-spun and annealed fibers, likewise.

The observed segmental order parameters of $S_{Z'Z'}$ = 0.7 (mobile component) and $S_{Z'Z'}$ = 0.75 (immobile component) indicate highly extended chain conformations. Furthermore, orientational order parameters of S_{ZZ} = 0.9 reflect a large measure of parallel orientation of the mesogenic units. Finally, melt spinning produces fibers with practically all director axes aligned in draw direction, evidenced by a macroorder parameter of $S_{z''z''}$ = 0.9. Note, however, that this value still increases with decreasing spinning temperature to $S_{z''z''} > 0.95$.

In summary, melt spun fibers of the LCP I exhibit exceptionally high order parameters on the different molecular levels. High modulus and strength result from the highly oriented chain configurations, as we shall see in the next paragraph.

Tensile Properties. Table II summarizes the mechanical properties of annealed fibers of LCP I. The data indicate surprisingly high initial moduli of 11 GPa $\leq E \leq$ 22 GPa, tensile strengths up to T = 0.34 GPa, and elongation to break ratios of ϵ = 2.5%. At present, these data seem to be the best values reported on LCPs containing flexible spacers of comparable lengths.

Please note the effect of the molecular weight on the tensile strength T, leading to an increase of T with the degree of polymerization. In contrast, the Young modulus

E is independent of the molecular weight within the range investigated. However, E can be increased by lowering the spinning temperature T_s. In fact, the highest modulus was obtained for fibers spun only 8 K above the melting point.

Discussion

The mechanical behavior of fibers is strongly correlated to their properties on the molecular level. A variety of experimental methods have been employed to obtain such information.[36-39] The present knowledge about the molecular structure of fibers originates to a large extent from X-ray diffraction studies.[8,9,40] In addition, NMR line-shape investigations have been used to provide information about the molecular organization of these systems.[13,41,42] This approach is useful for examining orientational and conformational order of the polymer chains and slow molecular motions in certain polymer phases. For a complete dynamic characterization, however, comprehensive relaxation studies[7,43] are required. In the following, molecular order and dynamics will be discussed separately.

Molecular Dynamics of Fibers. Depending on the thermal history, the molecular dynamics of as-spun and annealed fibers is significantly different. The results for the annealed fibers (see Figure 5) indicate surprisingly fast chain dynamics in these "solid" fibers. Note that this detailed information could be obtained only by employing pulsed dynamic NMR techniques. For any given temperature two different relaxation experiments were carried out.

The heterogeneity of the annealed fibers is reflected in their dynamic behavior. Two components are observed, which we assign to a liquid-crystalline (mobile component) and a crystalline phase (immobile component). The assignment is confirmed by the thermogram of the fibers (see Figure 1c), showing a glass and a melt transition. Note, however, that the enthalpy of fusion (see Table I) is lower than observed in conventional semicrystalline polymers,[44,45] suggesting a decreased regularity of the crystalline regions. Similar observations are reported for other LCPs.[46,47]

Decomposition of various NMR relaxation curves into two components yields a fiber crystallinity of (55 ± 5)%, subject to the annealing conditions (see Experimental Section). Whereas the dynamics of the crystalline component is characterized by slow conformational changes, the liquid-crystalline regions also exhibit intermolecular motions with correlation times up to 10^{-8} s. However, the Arrhenius plot for these overall motions is not linear, the apparent activation energies increasing with decreasing temperature. Thus, all intermolecular motions gradually freeze and at temperatures $T < T_g$ intramolecular motions are the dominant process. In fact, we have been able to detect trans–gauche isomerization even at $T = 130$ K with a correlation time of $\tau_J = 10^{-4}$ s. Similarly, ring flips and chain isomerization could be followed down to temperatures 100 K below the glass transition.[41,48,49]

Figure 5 clearly shows the coexistence of liquid-crystalline and crystalline components, differing drastically in their molecular dynamics. In that respect fibers from LCPs resemble those from ordinary polymers, which exhibit amorphous and crystalline phases. However, a broad distribution of correlation times is generally evaluated in all but the lowest molecular weight systems.[42,48] In contrast, molecular reorientation in the LCP fibers appears to occur essentially by single processes, where any distribution of correlation times must be restricted to less than one decade. It should be noted that these results are consistent with observations on bulk samples, which were slowly cooled from the nematic melt.[7,43,50]

Let us now discuss the molecular dynamics of as-spun fibers, not yet evaluated in detail. A preliminary analysis indicates only a single component, exhibiting a chain mobility comparable to that of the liquid-crystalline regions. On the other hand, the DSC thermogram of as-spun fibers (see Figure 1b) clearly shows the existence of a crystalline component. The contradictory results can be reconciled by considering the spinning experiment, in which the LCP is quenched from the nematic melt to the solid state. It is suggested that during the short cooling period only small crystals are formed, unable to give distinct NMR signals but organized enough to yield heats of transition. Annealing of the LCP fibers at elevated temperatures then leads to a better development of the crystalline regions, necessary for proper NMR detection.

From X-ray diffraction studies of thermotropic copolymers it was concluded that annealing causes an improvement of the ordered structure both in terms of an increasing registry of the chain molecules and an increase of the degree of crystallization.[46] The latter effect is essentially confirmed by our annealing experiments on the LCP I. For example, in the DSC curve of as-spun fibers the low-temperature endotherm (see Figure 1b) is caused by an annealing process at room temperature. By further annealing at higher temperatures this endotherm disappears whereas a new endotherm approximately 15 K above the annealing temperature can be detected (see Figure 1c). This behavior, observed for other semicrystalline polymers,[51-54] can be explained by fusion of the low-temperature crystals and subsequent formation of new crystallites stable at the higher annealing temperature. In summary, we conclude that the degree of crystallinity evaluated from the NMR relaxation experiments comprises the original high-temperature crystallization and the subsequent postcrystallization (about 25%) upon annealing.

Molecular Order of Fibers. A particular advantage of the dynamic NMR studies, presented in this paper, is the possibility to discriminate between different types of molecular order, i.e., to separate conformational, orientational, and macroorder of the chains (see Table II).

The observed segmental order parameter $S_{Z'Z'} = 0.7$ in the liquid-crystalline phase is practically independent of the position within the spacer.[7,50,55] Evidently, highly extended conformers prevail in the nematic phase of LCP I. This finding, which is corroborated by ^{2}H NMR studies of other thermotropic polyesters,[56,57] is the most prominent feature distinguishing liquid-crystal main-chain polymers from side-chain polymers[58] and their monomeric analogues.[59-61] Predictions of statistical mechanical theories,[62,63] developed for these polymers, are in qualitative agreement with the NMR results. It appears that a number of unique properties, exhibited by semiflexible main-chain polymers, can be attributed to the conformational order which is restricted to highly extended configurations.

On the other hand, the crystalline component shows a segmental order parameter of $S_{Z'Z'} = 0.75$, far below the limiting value of $S_{Z'Z'} = 1.0$ expected for a regular crystal. This finding corresponds to the minor enthalpy of fusion (see Table I), being considerably smaller than that of conventional semicrystalline polymers.[44,45] Apparently, the regularity of the crystalline regions[46,47] is reduced by conformational disorder of the spacer, as described previously.[7,50]

Inspection of Table II also reveals a high value for the orientational order parameter of $S_{ZZ} = 0.9$, independent of temperature and thermal history. The observed value is considerably larger than that exhibited by low molecular weight nematogens.[59-61] As predicted[62-64] the polymer chains are highly ordered on a molecular level in agreement with ESR[65] and ^{1}H NMR studies.[66,67]

Finally, let us discuss the macroorder parameter $S_{z''z''}$, characterizing the alignment of the director axes with respect to the draw direction. Table II shows extraordinary high values of $S_{z''z''} \geq 0.9$, depending on the spinning conditions. Evidently, the spinning temperature is a crucial parameter. For example, spinning at $T_s - T_m = 8$ K increases $S_{z''z''}$ to $S_{z''z''} > 0.95$, due to an increase in melt viscosity, as will be discussed in the next section. It should be noted, however, that similarly high macroorder parameters were achieved by using other orientation methods such as strong magnetic fields or solid-state extrusion.[43,50,65]

Summing up, the molecular structure of the LCP fibers is characterized by a high degree of conformational and orientational order of the polymer chains. In addition, practically all director axes are aligned in the draw direction. Annealing of the fibers results in a better development of the crystalline regions without any significant improvement of the degree of order. These findings present the molecular basis for the unusual mechanical properties discussed in the next section.

Mechanical Properties of Fibers. The tensile properties reported in Table II are considerably better than those observed previously for similar systems.[11,12] From our spinning experiments a dependence of these properties on molecular weight and spinning temperature can be derived. As expected,[68] the tensile strength increases with the degree of polymerization. In contrast, the initial modulus is independent of molecular weight in the range of $10\,000 \leq \bar{M}_n \leq 30\,000$. It should be noted, however, that below $\bar{M}_n = 9000$ melt spinning is impossible, due to a break of the filaments under their own weight. As reported earlier, fibers from low molecular weight samples can be produced by solid-state extrusion.[65]

The effect of the spinning temperature T_s is clearly visible for the tensile modulus which increases by lowering T_s. Generally, high viscosities are required to maintain the macroscopic alignment while the fibers are cooling.[69-72] Rheological measurements on LCP I indicate a strong increase in melt viscosity with decreasing temperature leading to an optimum spinning temperature of $5 \text{ K} \leq T_s - T_m \leq 15$ K.[73] Table II clearly shows an increase in alignment and initial modulus with decreasing temperature. Thus, the highest modulus of $E = 22$ GPa is found for fibers that were spun just 8 K above the melting point. Generally, the observed mechanical properties are at least comparable or even better than those obtained for conventional posttreated polymer fibers.

Annealing of the LCP fibers only has a minor effect on the mechanical properties, in contrast to observations on other thermotropic polyesters.[74] This finding can be rationalized by the high degree of order, already exhibited by the as-spun fibers. A slight increase in tensile strength observed upon annealing may be caused by a better development of the crystalline regions.

The elongation to break ratios of $2\% \leq \epsilon \leq 3\%$ are considerably smaller than those evaluated for fibers of nonmesomorphic polymers.[3] Apparently, in the LCP fibers the polymer chains are in an extended[7] and oriented state,[75] which prevents further drawing.

Let us now speculate on the improvement of the mechanical properties. First of all, increasing the molecular weight of the samples, possibly by melt polymerization, should increase the tensile strength of the fibers. Furthermore, an improved sample homogeneity along the fibers is required for higher modulus and strength. This can be achieved by using larger quantities of the polymer in the spinning experiment. The use of specifically deuteriated polymers restricted the amount of material available for each run. Finally, we expect that shortening of the flexible spacer increases the conformational order and thus improves the mechanical properties. As deduced from the NMR experiments, the long aliphatic chain of LCP I introduces a certain amount of conformational disorder, which apparently restricts the achievable tensile properties.

Conclusions

Pulsed dynamic NMR of fibers from semiflexible LCPs has provided detailed information about molecular order and dynamics of these systems. The results, referring to as-spun and annealed fibers, have been discussed in relation to the tensile properties, evaluated by mechanical measurements. Principal conclusions that emerge from this combined study are the following:

(1) Molecular motion in the "solid" fibers is surprisingly fast but heterogeneous, as two components are observed, which we assign to a liquid-crystalline and a crystalline phase. The degree of crystallinity, evaluated from the NMR experiments, comprises the original crystallization during melt spinning and the subsequent postcrystallization upon annealing.

(2) Molecular structure of the fibers is characterized by a high degree of conformational and orientational order of the polymer chains. In addition, practically all director axes are aligned in the draw direction. Annealing results in a better development of the crystalline regions without any significant improvement of the degree of order.

(3) The mechanical properties of the fibers are strongly correlated to their properties on the molecular level. As expected, high modulus and strength result from the highly oriented chain configurations. It is suggested that improvement of the mechanical properties can be achieved by a systematic variation of the molecular structure.

In summary, pulsed dynamic NMR in combination with an appropriate relaxation model presents a powerful tool for characterizing new evolving materials such as LCP fibers.

Acknowledgment. It is a pleasure to thank Dr. B. Hisgen (BASF, Ludwigshafen) for his advice and help in the mechanical measurements. We are also grateful to Professor H. Herlinger and K. H. Wiese (Textil und Faserforschung, Stuttgart) for assistance in fiber spinning and characterization. Financial support of this work by the Deutsche Forschungsgemeinschaft and Fond der Chemischen Industrie is gratefully acknowledged.

Registry No. I (copolymer), 110374-61-3; I (SRU), 100753-66-0.

References and Notes

(1) White, J. L.; Fellers, J. F. *J. Appl. Polym. Sci. Symp.* **1978**, *33*, 137.
(2) Dobb, M. G.; McIntyre, J. E. *Adv. Polym. Sci.* **1984**, *60/61*, 61.
(3) Chung, T.-S. *Polym. Eng. Sci.* **1986**, *26*, 901.
(4) Prevorsek, D. C. In *Polymer Liquid Crystals*; Ciferri, A., Krigbaum, W. R., Meyer, R. B., Eds.; Academic: New York, 1982; p 329.
(5) Jackson, W. J.; Kuhfuss, H. F. *J. Polym. Sci., Polym. Chem. Ed.* **1976**, *14*, 2043.
(6) Ober, Ch. K.; Jin, J.-I.; Lenz, R. W. *Adv. Polym. Sci.* **1984**, *59*, 103.
(7) Müller, K.; Meier, P.; Kothe, G. *Progr. Nucl. Magn. Reson. Spectrosc.* **1985**, *17*, 211.
(8) Mitchell, G. R.; Windle, A. H. *Polymer* **1983**, *24*, 1513.
(9) Chivers, R. A.; Blackwell, J. *Polymer* **1985**, *26*, 997.
(10) Muramatsu, H.; Krigbaum, W. R. *J. Polym. Sci., Polym. Phys. Ed.* **1986**, *24*, 1695.
(11) Blumstein, A.; Vilasagar, S.; Ponrathnam, S.; Clough, S. B.; Blumstein, R. B. *J. Polym. Sci., Polym. Phys. Ed.* **1982**, *20*, 877.

(12) Acierno, D.; La Mantia, F. P.; Polizotti, G.; Ciferri, A.; Krigbaum, W. R.; Kotek, R. *J. Polym. Sci., Polym. Phys. Ed.* **1983**, *21*, 2027.
(13) Spiess, H. W. In *Developments in Oriented Polymers*; Ward, I. M., Ed.; Applied *Science Publishers*: London **1982**; p 47.
(14) Bovey, F. A.; Jelinski, L. W. *J. Phys. Chem.* **1985**, *89*, 571.
(15) Meier, P.; Ohmes, E.; Kothe, G. *J. Chem. Phys.* **1986**, *85*, 3598.
(16) Kubo, R. In *Advances in Chemical Physics*; Shuler, K., Ed.; Wiley: New York, 1969; Vol. 16, p 101.
(17) Freed, J. H.; Bruno, G. V.; Polnaszek, C. F. *J. Phys. Chem.* **1971**, *75*, 3385.
(18) Norris, J. R.; Weissman, S. I. *J. Phys. Chem.* **1969**, *73*, 3119.
(19) Kothe, G. *Mol. Phys.* **1977**, *33*, 147.
(20) Flory, P. J. *Statistical Mechanics of Chain Molecules*; Interscience Publishers: New York, 1969.
(21) Cotter, M. A. *J. Chem. Phys.* **1977**, *66*, 1098.
(22) Saupe, A. *Z. Naturforsch.* **1964**, *19A*, 161.
(23) Müller, K.; Eisenbach, C.; Hisgen, B.; Ringsdorf, H.; Schneller, A.; Lenz, R. W.; Kothe, G., unpublished results.
(24) Jin, J.-I.; Antoun, S.; Ober, C.; Lenz, R. W. *Br. Polym. J.* **1980**, 132.
(25) Antoun, S.; Lenz, R. W.; Jin, J.-I. *J. Polym. Sci., Polym. Chem. Ed.* **1981**, *19*, 1901.
(26) Powles, J. G.; Strange, J. H. *Proc. Phys. Soc.* **1963**, *82*, 6.
(27) Davis, J. H.; Jeffrey, K. R.; Bloom, M.; Valic, M. F.; Higgs, T. P. *Chem. Phys. Lett.* **1976**, *42*, 390.
(28) Meier, P.; Ohmes, E.; Kothe, G.; Blume, A.; Weidner, J.; Eibl, H.-J. *J. Phys. Chem.* **1983**, *87*, 4904.
(29) Cholli, A. L.; Dumais, J. J.; Engel, A. K.; Jelinski, L. W. *Macromolecules* **1984**, *17*, 2399.
(30) Hentschel, R.; Spiess, H. W. *J. Magn. Reson.* **1979**, *35*, 157.
(31) Bloom, M.; Davis, J. H.; Valic, M. I. *Can. J. Phys.* **1980**, *58*, 1510.
(32) Gordon, R. G.; Messenger, T. In *Electron Spin Relaxation in Liquids*; Muus, L. T., Atkins, P. W., Eds.; Plenum: New York, 1972; p 341.
(33) Moro, G.; Freed, J. H. *J. Chem. Phys.* **1981**, *74*, 3757.
(34) Redfield, A. G. *Adv. Magn. Reson.* **1965**, *1*, 1.
(35) Kohlhammer, K.; Müller, K.; Kothe, G., unpublished results.
(36) Ward, I. M. *Structure and Properties of Oriented Polymers*; Applied Science Publishers: *London*, 1975.
(37) Ward, I. M., Ed. *Developments in Oriented Polymers*; Applied Science Publishers: London, 1982.
(38) Ward, I. M. *Adv. Polym. Sci.* **1985**, *66*, 81.
(39) Monnerie, L. *Pure Appl. Chem.* **1985**, *57*, 1563.
(40) Windle, A. H. In *Developments in Oriented Polymers*; Ward, I. M., Ed.; Applied Science Publishers: London, 1982; p 1.
(41) Hentschel, R.; Sillescu, H.; Spiess, H. W. *Polymer* **1981**, *22*, 1516.
(42) Spiess, H. W. *Adv. Polym. Sci.* **1985**, *66*, 23.
(43) Müller, K.; Hisgen, B.; Ringsdorf, H.; Lenz, R. W.; Kothe, G. *Mol. Cryst. Liq. Cryst.* **1984**, *113*, 167.
(44) Wunderlich, B. *Macromol. Phys.* Academic: New York, 1980; Vol. 1–3.
(45) Wunderlich, B.; Grebowicz, J. *Adv. Polym. Sci.* **1984**, *60/61*, 1.
(46) Butzbach, G. D.; Wendorff, J. H.; Zimmermann, H. J. *Polymer* **1986**, *27*, 1337.
(47) Wendorff, J. H.; Zimmermann, H. J. *Angew. Makrom. Chem.* **1986**, *145/146*, 231.
(48) McBrierty, V. J.; Douglass, D. C. *J. Polym. Sci., Macromol. Rev.* **1981**, *16*, 295.
(49) Kintanar, A.; Jelinski, L. W.; Gancarz, I.; Koberstein, J. T. *Macromolecules* **1986**, *19*, 1876.
(50) Müller, K.; Kothe, G. *Ber. Bunsenges. Phys. Chem.* **1985**, *89*, 1214.
(51) Illers, K.-H. *Makromol. Chem.* **1969**, *127*, 1.
(52) Cheng, S. Z. D.; Cao, M.-Y.; Wunderlich, B. *Macromolecules* **1986**, *19*, 1868.
(53) Windle, A. H.; Viney, C.; Golombok, R.; Donald, A. M.; Mitchell, G. R. *Faraday Discuss. Chem. Soc.* **1985**, *79*, 55.
(54) Gochanour, C. R.; Weinberg, M. *J. Rheol.* **1986**, *30*, 101.
(55) Müller, K.; Hisgen, B.; Ringsdorf, H.; Lenz, R. W.; Kothe, G. In *Recent Advances in Liquid Crystalline Polymers*; Chapoy, L. L., Ed.; Elsevier Applied Science Publishers: London, 1985; p 223.
(56) Samulski, E. T.; Gauthier, M. M.; Blumstein, R. B.; Blumstein, A. *Macromolecules* **1984**, *17*, 479.
(57) Yoon, D. Y.; Bruckner, S.; Volksen, W.; Scott, J. C.; Griffin, A. C. *Faraday Discuss. Chem. Soc.* **1985**, *79*, 41.
(58) Wassmer, K.-H.; Ohmes, E.; Portugall, M.; Ringsdorf, H.; Kothe, G. *J. Am. Chem. Soc.* **1985**, *107*, 1511.
(59) Hsi, S.; Zimmermann, H.; Luz, Z. *J. Chem. Phys.* **1978**, *69*, 4126.
(60) Emsley, J. W.; Luckhurst, G. R.; Stockley, C. P. *Proc. R. Soc. London, Ser. A* **1982**, *381*, 117.
(61) Samulski, E. T. *Isr. J. Chem.* **1983**, *23*, 329.
(62) Abe, A. *Macromolecules* **1984**, *17*, 2280.
(63) Yoon, D. Y.; Bruckner, S. *Macromolecules* **1985**, *18*, 651.
(64) Ronca, G.; Yoon, D. Y. *J. Chem. Phys.* **1982**, *76*, 3295; **1984**, *80*, 925.
(65) Müller, K.; Wassmer, K.-H.; Lenz, R. W.; Kothe, G. *J. Polym. Sci., Polym. Lett. Ed.* **1983**, *21*, 785.
(66) Martins, A. F.; Ferreira, J. B.; Volino, F.; Blumstein, A.; Blumstein, R. B. *Macromolecules* **1983**, *16*, 279.
(67) Blumstein, R. B.; Stickles, E. M.; Gauthier, M. M.; Blumstein, A.; Volino, F. *Macromolecules* **1984**, *17*, 177.
(68) Termonia, Y.; Meakin, P.; Smith, P. *Macromolecules* **1985**, *18*, 2246.
(69) Jackson, W. J. *Br. Polym. J.* **1980**, *12*, 154.
(70) Jackson, W. J. *Macromolecules* **1983**, *16*, 1027.
(71) Ide, Y.; Chung, T.-S. *J. Macromol. Sci. Phys.* **1984–1985**, *B23*, 497.
(72) Huynh-Ba, G.; Cluff, E. F.; In *Polymeric Liquid Crystals*; Blumstein, A., Ed.; Plenum: New York, 1985; p 217.
(73) Schleicher, A. Diploma Thesis, Stuttgart, 1985.
(74) Kwolek, S. L.; Luise, R. R. *Macromolecules* **1986**, *19*, 1789.
(75) Stamatoff, J. B. *Mol. Cryst. Liq. Cryst.* **1984**, *110*, 75.